(BL21 cells) transformed with pGPF, and the fusion protein was purified by using sequentially both Glutathione Sepharose 4B (Pharmacia Biotech) and anti-Flag M2 affinity gel (Eastman Kodak) beads. This protein was used only for RBSS experiments (Fig. 1A). His_6:PIF3, G:bhPIF3, and phyB proteins were produced by transcription and translation (TnT) systems (Promega). PIF3 coding sequence was amplified by PCR and cloned into pRSETb vector (Invitrogen). The resulting fusion protein contains a His_6-tag at the NH_2-terminal end and was used throughout the work (referred to as PIF3 in the figures). G:bhPIF3 corresponds to GST (glutathione S-transferase) (Fig. 1D, gray box) fused to the PIF3 bHLH domain (from residue 340 to 397; cross-hatched box). The PIF3 bHLH domain was amplified by PCR and cloned in pGEX-4T-1. The resulting coding region was amplified with oligonucleotides that added the T7 promoter sequence upstream of the first ATG, and the PCR product was directly used as a template in the TnT reaction. The full-length *Arabidopsis* PHYB apoprotein was produced by TnT reaction, and the chromophore was autocatalytically attached (*28*).

43. The binding reactions were performed essentially as described [J. F. Martínez-García and P. H. Quail, *Plant J.* **18**, 173 (1999)] with modifications. The binding buffer was supplemented with 10% glycerol and 0.05% NP-40, and nonspecific competitor used was 50 ng of poly(dI-dC). poly(dI-dC) per reaction. The binding complexes were resolved by EMSAs in 4% polyacrylamide gel in 0.5× tris-borate EDTA buffer at room temperature (90 min at 10 V cm^{-1}), and the gels were dried and autoradiographed.
44. F. R. Cantón and P. H. Quail, *Plant Physiol.* **121**, 1207 (1999).
45. RBSS was performed as described [T. K. Blackwell and H. Weintraub, *Science* **250**, 1104 (1990)] with modifications. We synthesized 60-base oligonucleotides of which the middle 12 bases consisted of random sequences (5′-GTCTGTCTGGATCCGAGGTGAGTA-N12-ACGTCTTCCGAAGCTTACGTCGCG-3′). Two 20-base oligonucleotides were also synthesized as forward (5′-GTCTGTCTGGATCCGAGGTG-3′) and reverse (5′-CGCGACGTAAGCTTCGGAAG-3′) primers. The stringency of RBSS was increased by increasing the amount of nonspecific competitor (50, 100, 200, 400, and 500 ng, from first to fifth cycles, respectively) and by decreasing the amount of protein [2, 2, 1, 1, and 1 μl of TnT-expressed PIF3 (*42*), or 500, 500, 500, 250, and 250 ng of *E. coli*–purified GST:PIF3:flag protein (*42*), from first to fifth cycle, respectively] and the amount of labeled DNA probe [90,000 cpm (~10^6 cpm μg^{-1}) for the first round; 20,000 cpm of high-specific activity probe from second to fifth cycle] in the binding reaction (*43*). After five rounds of selection, the retarded DNA was amplified by PCR, digested with Bam HI–Hind III, and cloned into pBluescript. Individual clones were randomly selected and sequenced. The sequences were aligned centered around the identified G-box motif.
46. Light sources are described in (*28*). Pulses were 2 min of FR (88 μmol m^{-2} s^{-1}) or R light (88 μmol m^{-2} s^{-1}).
47. The selected LREs used [GT1, 4× (5′-TGTGTGGTTAATATG-3′); Z, 2× (5′-ATCTATTCGTATACGTGTCAC-3′); G, 4× (5′-TGACACGTGGCA-3′); and GATA, 4× (5′-AAGATAAGATT-3′)] have been described elsewhere (*33*).
48. After germination, seedlings were grown in the dark at 22°C for 4 days. Material was harvested at various times after 0, 1, 2, 3, and 4 hours of exposure to continuous red light (Rc; 20 μmol m^{-2} s^{-1}). Total RNA was isolated with the RNeasy Plant Miniprep kit (Qiagen). For RNA analyses, 5 μg of total RNA were loaded per lane, and then transferred to MSI Nylon membranes. The membranes were hybridized in Church buffer at 65°C overnight with random primer–labeled fragments (*CCA1*, *LHY*, *CHS*, *SPA1*). *CCA1* and *LHY* probes were amplified by PCR from *Arabidopsis* DNA with the use of specific primers, cloned, and confirmed by sequencing. The *CCA1* probe (amplified with the primers 5′-GCAGCTGCTAGTGCTTGGTGGGCT-3′ and 5′-TCATGTGGAAGCTTGAGTTTCCAA-3′) corresponded to positions 2082 to 3010 in the 3′ region of the main open reading frame (ORF) (*38*, *39*); the *LHY* probe (amplified with the primers 5′-CATGCTGCAGCTACATTCGCTGCT-3′ and 5′-TCATGTAGAAGCTTCTCCTTCCAATCG-3′) corresponded to positions 1271 to 2275 in the 3′ region of the main ORF (*40*). Southern blot analysis showed no detectable cross-hybridization between *CCA1* and *LHY* probes under the washing conditions used (*34*). The *SPA1* (*14*) and *CHS* [R. L. Feinbaum and F. M. Ausubel, *Mol. Cell. Biol.* **8**, 1985 (1988)] probes have been described elsewhere.
49. Relative levels of transcripts were normalized to 18*S* ribosomal RNA levels (*44*) after PhosphorImager Storm 860 (Molecular Dynamics) quantification.
50. We thank Y. Kang for technical assistance; M. Ni for A22 seeds and original PIF3 clones; C. Fairchild for the phycocyanobilin; U. Hoecker for SPA1 cDNA; N. Wei for the *CHS* probe; E. Monte and M. Rodríguez-Concepción for support and discussion; all the lab members for discussion and support; and the *Arabidopsis* Biological Resource Center (Columbus, Ohio) for providing *hy5* (hy5-1 allele) seeds. Supported by grants from the U.S. Department of Energy Basic Energy Sciences (DE-FG03-87ER13742) and U.S. Department of Agriculture Current Research Information Service (5335-21000-010-00D).

13 December 1999; accepted 25 February 2000

Template Boundary in a Yeast Telomerase Specified by RNA Structure

Yehuda Tzfati, Tracy B. Fulton, Jagoree Roy, Elizabeth H. Blackburn*

The telomerase ribonucleoprotein has a phylogenetically divergent RNA subunit, which contains a short template for telomeric DNA synthesis. To understand how telomerase RNA participates in mechanistic aspects of telomere synthesis, we studied a conserved secondary structure adjacent to the template. Disruption of this structure caused DNA synthesis to proceed beyond the normal template boundary, resulting in altered telomere sequences, telomere shortening, and cellular growth defects. Compensatory mutations restored normal telomerase function. Thus, the RNA structure, rather than its sequence, specifies the template boundary. This study reveals a specific function for an RNA structure in the enzymatic action of telomerase.

Telomerase, a ribonucleoprotein reverse transcriptase (RT), replenishes telomeric DNA that would otherwise be lost with each round of eukaryotic DNA replication (*1*). The telomerase complex contains an RNA subunit (TER), a catalytic RT protein (TERT), and several additional protein components (*2*). Telomerase is activated in most human cancers, and its ectopic expression can greatly extend the life-span of normal human cells in culture (*3*).

Telomerase RNAs are extremely divergent in sequence and vary in length from 146 nucleotides (nt) in the ciliate *Tetrahymena paravorax* (*4*) to 1544 nt in the budding yeast *Candida albicans* (*5*). Unlike other RTs, which perform extensive genome copying, telomerase copies only a small portion (termed the "template") of an intrinsic RNA moiety (*6*). This feature allows telomerase to synthesize onto telomeres a species-specific, 5- to 26-base-long repeated sequence (*7*). How telomerase specifies its template boundaries (where DNA synthesis initiates and where it ends on the TER sequence) is not understood.

Nontemplate regions have been previously shown to be required for telomerase activity (*8*, *9*) and ribonucleoprotein (RNP) assembly (*9*, *10*). To further investigate the participation of telomerase RNA in the enzymatic function of telomerase, we searched for conserved sequences and structural elements in budding yeast telomerase RNAs. We cloned and analyzed TER genes from four *Kluyveromyces* species closely related to *K. lactis* (*11*). The mature RNAs ranged in length from 930 nt in *K. aestuarii* to 1320 nt in *K. dobzhanskii*. Sequence identity between any given pair of genes ranged from insignificant to about 70% overall identity. The computer program *mfold* (*12*) predicted extensive secondary structures for these RNA sequences, including a common feature shared by all five TERs: base pairing of the sequence immediately upstream of the template (pairing element B) (Fig. 1A) with a sequence 200 to 350 nt further upstream (pairing element A), located near the 5′ end of the RNA. The region between the pairing elements (indicated by the dashed line in Fig. 1A and the dashed loop in Fig. 1B) was shown previously to be dispensable in *K. lactis* (*9*). The proximity of this conserved putative pairing region to the 5′ end of the template led us to hypothesize that its function is to limit DNA synthesis, thereby defining the downstream boundary of the template.

To test this hypothesis, we constructed a series of mutations in the putative pairing region of the *K. lactis* TER gene (Fig. 1, C and D). We replaced the wild-type TER gene in *K. lactis* with the mutant genes by a vector-shuf-

Department of Microbiology and Immunology, University of California, San Francisco, San Francisco, CA 94143–0414, USA.

*To whom correspondence should be addressed. E-mail: telomer@itsa.ucsf.edu

fling system described previously (*9*) and analyzed their effects in vitro and in vivo. In each of four disruption mutations (D1, D1′, D2, and D2′) (Fig. 1, C and D), a trinucleotide sequence within either strand of the pairing region was substituted with its complementary sequence. The D1 and D1′ mutations, in pairing elements A and B, respectively, were designed to unwind the first 3 base pairs (bp) of the putative pairing region, adjacent to the template. The D2 and D2′ mutations targeted 3 bp in the middle of pairing elements A and B, respectively, and were predicted to cause a more extensive disruption of the pairing. Pairing potential was restored in the double mutants D1/D1′ and D2/D2′. In a full replacement mutant, R1, 10 nt on each strand of the pairing region were replaced with unrelated sequences that maintained the original base composition and pairing potential (Fig. 1, C and D).

We next studied the effects of the pairing mutations on telomerase function, by assaying partially purified extracts from wild-type or mutant cells for telomerase activity in vitro (*13*). The characteristic pattern of elongation products synthesized by telomerase with a wild-type pairing region (Fig. 2A, lane 2) was described previously (*14*). It includes a faint band, corresponding to the longest product that can result from one round of synthesis along the maximal potential template (open arrowhead), and stronger bands, which are 1 to 3 nt shorter. The activities from each of the various cell extracts were ribonuclease A–sensitive (Fig. 2A, lane 1) (*15*), a hallmark of telomerase activity.

Strikingly, all the pairing-disruption mutants synthesized longer products than wild-type telomerase (Fig. 2A, compare lanes 4, 6, and 12 to lane 2; see also Fig. 2B, lanes 5 and 7). The D1 and D1′ mutations each resulted in detectable read-through of 2 nt (Fig. 2A, lanes 4 and 6; Fig. 2B, lanes 3 and 1). Because extracts prepared from the D2 and D2′ mutants had reduced telomerase activity (Fig. 2A, lanes 10 to 13), we integrated the D2 and D2′ mutant TER genes into the genome by replacing the endogenous gene (*16*). The resulting strains, iD2 and iD2′, exhibited stronger telomerase activity in vitro, generating detectable products with up to seven and four read-through nucleotides (Fig. 2B, lanes 7 and 5), respectively. For all strains tested, the polymerization activity observed was specific to the telomerase template sequence, as indicated by experiments in which deoxyadenylate triphosphate (dATP) was omitted. The resulting −dATP products were of the length expected if telomerase elongated the correctly aligned primer and stopped just before the uridine that is the last nucleotide in the maximal possible template (Fig. 2A, −dATP lanes). The read-through products were correctly copied from the TER sequence 5′ of the template, as indicated by the pattern of bands when deoxycytidine triphosphate (dCTP) was omitted from the reactions. Telomerase activity of the D1′ but not the D1 mutant was limited by the omission of dCTP, as expected if the G-containing D1′ mutation was to be copied (Fig. 2B, see disappearance of a band in lane 2 compared with that indicated by V-shaped arrowhead in lane 1). The difference in mobility between the D1 and D1′ read-through products (Fig. 2B, lanes 1 and 3) was another indication that these mutant enzymes copied different nucleotides. Synthesis by the D2 mutant was also limited by the omission of dCTP, as expected from copying the wild-type sequence adjacent to the template (Fig. 2B, see disappearance of bands in lane 6 compared with those indicated by V-shaped arrowheads in lane 7).

The presence of sequence covariation in the pairing elements of the TER genes (Fig. 1B) suggested that base pairing, rather than a specific sequence, is required to specify the template boundary. Two different experiments support this prediction. First, the D1/D1′ and D2/D2′ compensatory mutations re-established a normal, wild-type–like boundary (Fig. 2A, lanes 8 and 14). Second, R1 telomerase, with complementary but scrambled pairing sequences, also retained a normal boundary (Fig. 2A, lane 16). Together, the results showed that disrupting the secondary structure causes template read-through, and that restoring base pairing with complementary mutations re-establishes the normal boundary.

We also tested the effects of these mutations in vivo. To distinguish telomeric repeats added by the mutant telomerases from repeats synthesized previously by the wild-type enzyme, we used an additional single-nucleotide mutation producing a Bcl I restriction site within the template sequence. This mutation is phenotypically silent but results in the incorporation of telomeric repeats containing a Bcl I restriction site onto telomeres (*9*), thus marking the action of the mutant enzyme. All the pairing-mutant telomerases were active in vivo, which is evident by the incorporation of Bcl I site containing telomeric repeats. These repeats were detected by differential hybridization of a Bcl I–specific probe to Southern blotted genomic DNA cut with Eco RI restriction endonuclease (Fig. 3A). Secondary digestion with Bcl I endonuclease shortened the Eco RI telomeric re-

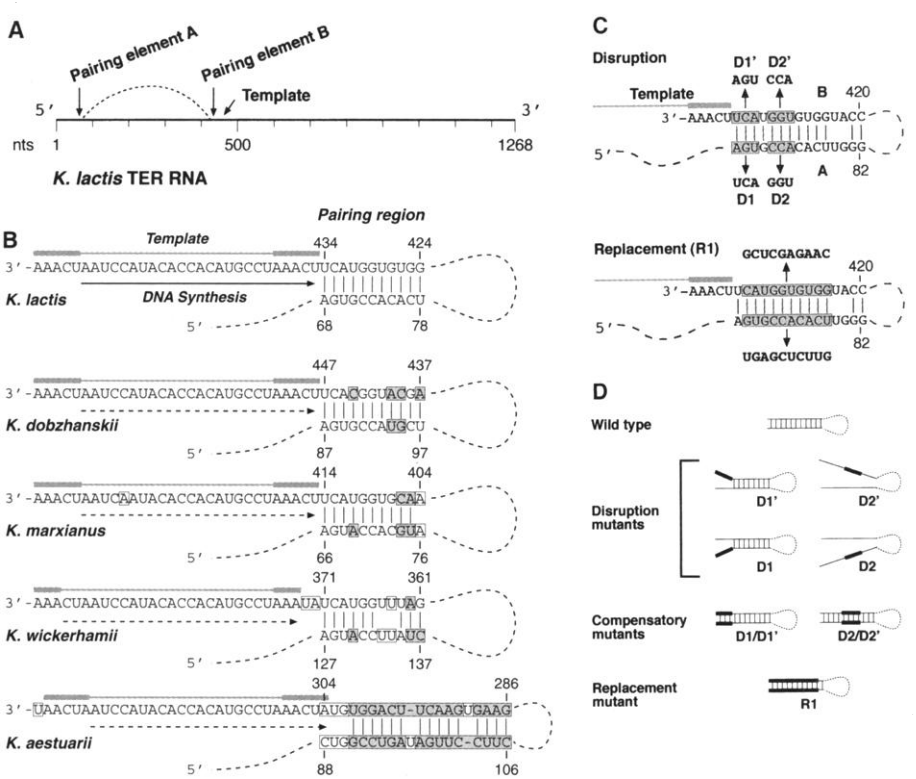

Fig. 1. Prediction of a pairing region in budding yeast telomerase RNAs. (**A**) A linear map of *K. lactis* TER illustrating the location of the template and the pairing elements A and B. (**B**) A pairing region, predicted by the computer program *mfold* (*12*), is located immediately upstream of the telomerase RNA template in five *Kluyveromyces* species. For each species, the horizontal gray line denotes the maximal putative template sequence, including the short repeated sequence at both ends (thick gray lines) thought to be required for realignment and synthesis of multiple telomeric repeats. Arrows indicate the direction of DNA polymerization along the template (solid arrow for the known template of *K. lactis*; dashed arrows for the putative templates of the newly cloned genes). Boxed nucleotides, sequence variation from the *K. lactis* TER gene; shaded boxed nucleotides, variations that retain the pairing potential. (**C**) Substitution mutations designed to test the pairing hypothesis in *K. lactis*. Shaded boxes, wild-type sequences that are substituted in the mutations. A and B are the pairing elements indicated in (A). (**D**) Effects of mutations within the pairing region, as predicted by the *mfold* program (*12*). Thick lines represent mutated sequences.

striction fragments, as detected by a wild-type probe (Fig. 3B), and eliminated the Bcl I–specific hybridization signal (Fig. 3A). The D1 and D1′ mutations, as well as the D1/D1′ double mutation, did not appear to affect telomere length or colony morphology (Fig. 3A). However, the D2 and D2′ telomeres (Fig. 3, A and B) and the iD2 and iD2′ telomeres (*17*) were considerably shortened, containing significantly fewer total telomeric repeats than wild-type telomeres, as indicated by the reduced hybridization intensity of the telomeric bands. This shortening correlated with rough colony appearance and longer population doubling times than that of the wild-type strain (*15*, *18*). In addition, two telomeric restriction fragments disappeared in each of the D2 and D2′ mutants (arrowheads, Fig. 3B) most likely through recombination in the subtelomeric region, which has been shown to be associated with impaired telomere maintenance (*18*).

The D2/D2′ and R1 mutants exhibited normal colony morphology and wild-type telomere length (Fig. 3A), consistent with their normal template boundary observed in vitro (Fig. 2, lanes 14 and 16). The lack of any apparent effect of the 20-base R1 substitution is striking in light of the severe defects in telomere maintenance and cell growth caused by the 3-base D2 or D2′ substitutions. Thus, base pairing at this region, rather than sequence, is important for telomere maintenance in vivo, supporting the results obtained in vitro.

To test whether nontelomeric read-through sequences were incorporated onto telomeres in vivo, we cloned and sequenced telomeres from each of the TER mutants with a new method designed to preserve any 3′ overhang of the telomere (*19*). At least 10 telomere clones were sequenced for each strain. In these clones, the average telomere length and the extent of Bcl I incorporation (*15*) matched the observations by Southern analyses (Fig. 3B), indicating that the polymerase chain reaction (PCR) products were representative of the telomere population.

In two of the D1 telomere clones (Fig. 3C) composed of the expected Bcl I–marked telomeric repeats (in green) distal to wild-type repeats (in blue), an extra A residue (in red) was found, embedded between two Bcl I repeats. Such a single additional A residue was unique to the D1 clones and was not found in any of the other (>130) wild-type and mutant telomere clones. The position of this A residue is consistent with DNA synthesis proceeding 1 nt beyond the normal template boundary in vivo. In vitro read-through occurred in 44% of the product molecules (see arrowheads, Fig. 2A, lane 4). The paucity of read-through sequences in the telomere clones may reflect less reading through in vivo, or removal of nontelomeric nucleotides (*20*). The D2 and D2′ telomere clones contained up to 11 read-through nucleotides incorporated onto telomeric termini (in red, Fig. 3C). In each case, the additional sequence was that predicted from copying by the mutant enzyme beyond the normal template boundary, including the D2′ mutation (boxed nucleotides). In contrast to the D1, D2, and D2′ clones, no read-through sequences were detected in any of the D1′ (*21*), D1/D1′, D2/D2′, and R1 clones (at least 10 different clones of each). Together, these results indicate that disrupting the pairing region causes template read-through not only in vitro, but also in vivo.

In summary, we have demonstrated that a phylogenetically conserved, long-range base-pairing interaction adjacent to the template in a yeast telomerase RNA specifies one boundary of the telomerase template, thus determining the end of the telomeric repeat synthesized. It is not known whether this mechanism of demarcating the template boundary is used in other telomerases. In ciliate TERs, a conserved sequence immediately upstream of the template has been proposed to play a role in specifying the template boundary (*22*). In *T. thermophila*, mutations at this region resulted in alteration of the template boundary, as revealed by an in vitro activity reconstitution assay (*23*). In *Saccharomyces cerevisiae*, a trinucleotide substitution introduced adjacent to the template caused telomerase to copy 1 nt beyond the normal boundary in vitro (*24*). Secondary structure predictions reveal a putative double-stranded element adjacent to the template of telomerase RNA in several other species, including *S. cerevisiae* and human (*15*). Whether these putative structures function similarly to the one described here is yet to be explored.

Local RNA secondary structures have been shown to cause pausing in DNA synthesis by retroviral RTs (*25*). Here, we report the utilization of a long-range RNA-RNA base-pairing interaction as a barrier for reverse transcription, specifying the telomerase template boundary. Hence, the special feature of telomerase—precise limitation of polymerization to the template—is achieved by an RNA-directed mechanism of the RNP enzyme and is not an inherent property of the telomerase RT protein. Such a direct function for TER in the enzymatic action of telomerase is consistent with an evolutionary scheme in which RNA enzymes, in an archaic RNA world, acquired protein components evolving into RNP enzymes (*26*). The RNA components then gradually lost their

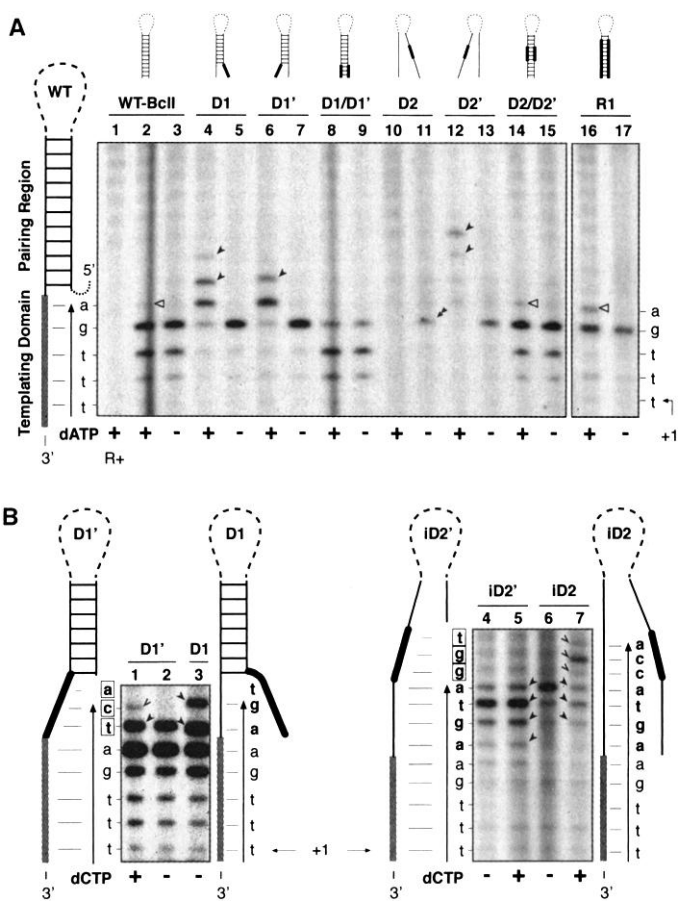

Fig. 2. Base-pairing disruption results in polymerization beyond the normal template boundary. *Kluyveromyces lactis* telomerase activity was assayed in vitro (*13*). All telomerases assayed contained a silent Bcl I mutation that is used to mark their action in vivo (see Fig. 3). **(A)** Telomerase reactions were incubated in the presence or absence of dATP, as indicated below the lanes. The predicted pairing region structures are illustrated above the lanes for each mutant. In lane 1 (R+), cell extract was pretreated with ribonuclease A (*14*). Open arrowheads, products ending at the last position of a template with a normal boundary; double arrowhead, a product of the D2 mutant enzyme observed upon omitting dATP; closed arrowheads, read-through products. **(B)** Reactions were incubated in the presence or absence of dCTP, as indicated below the lanes. V-shaped arrowheads highlight read-through products that disappear upon omitting dCTP from the reaction. Schematics on the sides of the panels illustrate polymerization along the template (thick gray line) with vertical arrows ending at the positions where the longest corresponding wild-type (A) or mutant (B) telomerase products were detected. Thick black lines, mutated TER sequences. The schematics show the nucleotides predicted to be incorporated at each position, starting at the first nucleotide added to the primer terminus. Read-through nucleotides are shown in bold. Nucleotides resulting from the predicted incorporation of the TER mutations are boxed.

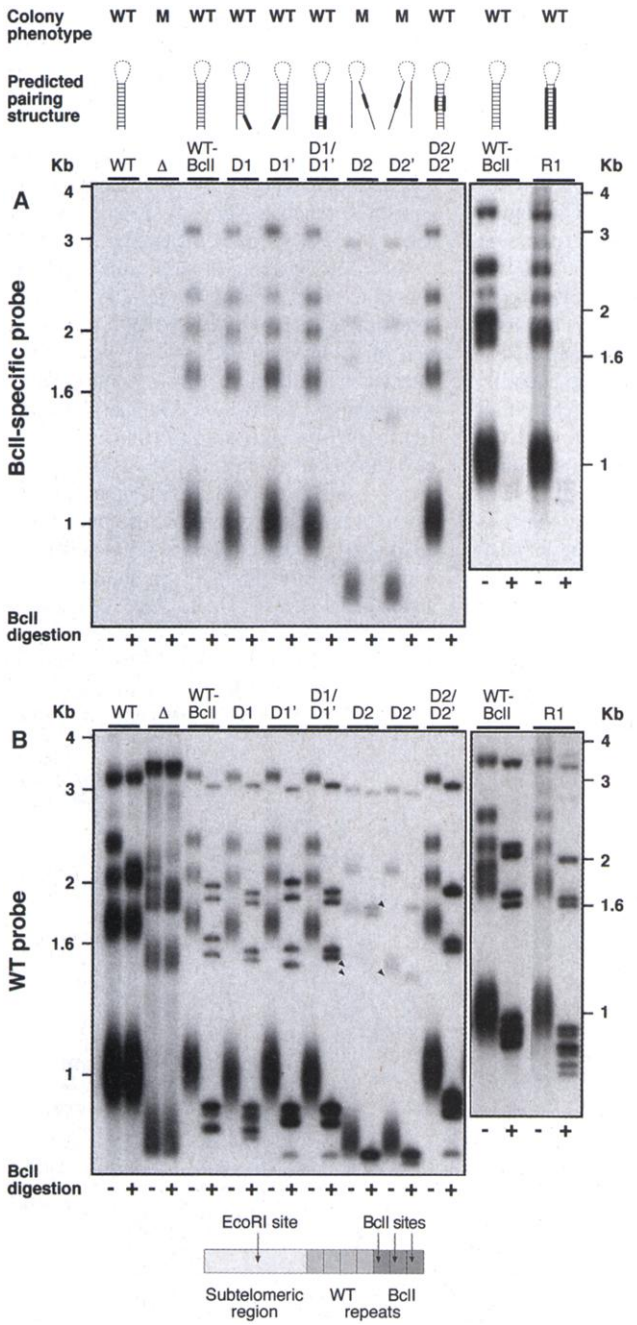

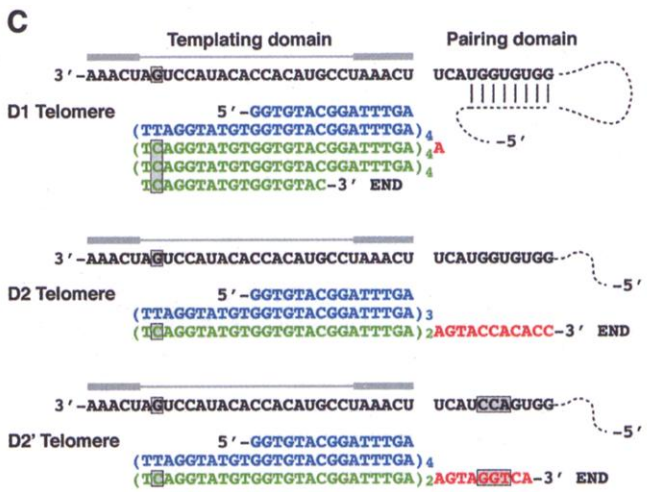

Fig. 3. Base-pairing disruption causes impaired telomere maintenance in vivo. Genomic DNA was prepared from *K. lactis* strains (deleted for the chromosomal TER gene and carrying the different TER alleles on a plasmid) at their 15th passage. The control strains carry on a plasmid a wild-type TER gene (WT), a Bcl I–marked (WT-Bcl I) TER gene, or no insert (Δ). DNA was digested with Eco RI restriction endonuclease (– lanes) or double-digested with Eco RI and Bcl I (+ lanes) and was then separated on 1% agarose gel and vacuum blotted. Blots were hybridized (*9*) with a Bcl I–specific oligonucleotide probe (**A**) and then with a wild-type telomeric sequence probe (**B**). Arrowheads indicate the expected location of telomeric restriction fragments that disappeared during cell divisions. The predicted pairing region structures are illustrated above the lanes in (A) for each mutant. Yeast colonies of the corresponding strains were examined under the microscope. Strains exhibiting the smooth wild-type colony phenotype are labeled WT; mutants exhibiting rough colony phenotype are labeled M (see text). The observed phenotype remained unchanged from the third passage (60 to 75 cell divisions) to the 15th passage (300 to 375 cell divisions). (**C**) Incorporation of Bcl I–marked repeats and read-through sequences onto telomeres in vivo. Sequence examples of telomere clones (*19*) are shown. Black, telomerase RNA sequences; blue, wild-type repeats; green, Bcl I–marked repeats; red, read-through sequences. Boxed, the Bcl I and the D2′ mutations in the RNA and the corresponding incorporated DNA sequences.

functional roles in catalysis and were subsequently dispensable. Telomerase RNP may represent an evolutionary relic—an intermediate in the transition from RNA replicases to protein reverse transcriptases (*27*). Further study of functional elements in TER will shed more light on telomerase evolution and function.

References and Notes

1. T. M. Bryan and T. R. Cech, *Curr. Opin. Cell Biol.* **11**, 318 (1999).
2. R. G. Weilbaecher and V. Lundblad, *Curr. Opin. Chem. Biol.* **3**, 573 (1999).
3. A. G. Bodnar *et al.*, *Science* **279**, 349 (1998); H. Vaziri and S. Benchimol, *Curr. Biol.* **8**, 279 (1998).
4. D. P. Romero and E. H. Blackburn, *Cell* **67**, 343 (1991).
5. E. Orr, M. J. McEachern, C. Strahl, Y. Tzfati, E. H. Blackburn, data not shown.
6. C. W. Greider and E. H. Blackburn, *Nature* **337**, 331 (1989).
7. E. Henderson, in *Telomeres*, E. H. Blackburn and C. W. Greider, Eds. (Cold Spring Harbor Laboratory Press, Cold Spring Harbor, NY, 1995), pp. 11–34.
8. C. Autexier, R. Pruzan, W. D. Funk, C. W. Greider, *EMBO J.* **15**, 5928 (1996); V. M. Tesmer *et al.*, *Mol. Cell. Biol.* **19**, 6207 (1999).
9. J. Roy, T. B. Fulton, E. H. Blackburn, *Genes Dev.* **12**, 3286 (1998).
10. J. R. Mitchell, J. Cheng, K. Collins, *Mol. Cell. Biol.* **19**, 567 (1999); A. G. Seto, A. J. Zaug, S. G. Sobel, S. L. Wolin, T. R. Cech, *Nature* **401**, 177 (1999).
11. *Kluyveromyces lactis* TER was cloned previously (*16*). Cloning of the other TER genes will be described elsewhere.
12. Secondary structures were predicted by the computer program *mfold* version 2.3 (*28*). The analyses were performed on the full-length wild-type and mutant TER sequences using the default parameters of the program except for the folding temperature, which was defined as 30°C.
13. Cells were grown in minimal medium to an optical density (OD) of 1 (plasmid-encoded TER alleles), then diluted 1:4 in yeast extract, peptone, and dextrose (YPD) medium, and grown to an OD of 2; or they were grown directly in YPD medium to an OD of 2 (integrated TER alleles). Telomerase activity in extracts from the homogenized cells (*9*) was partially purified and assayed as described (*14*). The primer used for all telomerase assays was 5′-GTGGTGTACGGA-3′.
14. T. B. Fulton and E. H. Blackburn, *Mol. Cell. Biol.* **18**, 4961 (1998).
15. Y. Tzfati, T. B. Fulton, E. H. Blackburn, unpublished material.
16. M. J. McEachern and E. H. Blackburn, *Nature* **376**, 403 (1995).
17. Y. Tzfati, T. B. Fulton, E. H. Blackburn, data not shown.
18. M. J. McEachern and E. H. Blackburn, *Genes Dev.* **10**, 1822 (1996).
19. Cloning of telomere fragments was modified from the ligation-anchored PCR strategy to clone RNA 5′ ends (*29*) as follows. Genomic DNA (0.5 μg) was ligated to a 5′-phosphorylated, 3′-NH_2-modified an-

chor oligonucleotide (Operon, Alameda, CA) at 37°C for 2 hours, followed by heat inactivation at 70°C for 15 min, then digestion with Eco RI restriction endonuclease, and purification with QIAquick PCR kit (Qiagen, Valencia, CA). The ligated DNA (150 ng) was amplified by PCR with an upper primer composed of a subtelomeric sequence present internally to 11 out of the 12 *K. lactis* telomeres (*15*) and an Apa I restriction site (5′-GACCGGGCCCAGCAGGACCAAG-3′), and a lower primer complementary to the anchor primer and containing an Eag I restriction site (5′-CGACGCGGCCGCTTATTAACCCT-3′). PCR products were extracted from an agarose gel, cloned into a Bluescript vector, and sequenced.

20. E. C. Greene, J. Bednenko, D. E. Shippen, *Mol. Cell. Biol.* **18**, 1544 (1998).
21. In the D1′ mutant, read-through of up to 3 nt would copy the D1′ mutation, resulting in the incorporation of 5′-TCA-3′. However, the same sequence would be incorporated at the beginning of another round of synthesis by the Bcl I–marked telomerase (see Fig. 3C). Therefore, limited read-through by the D1′ mutant enzyme may also have occurred in vivo but could not be distinguished from normal Bcl I telomeric repeats.
22. J. Lingner, L. L. Hendrick, T. R. Cech, *Genes Dev.* **8**, 1984 (1994).
23. C. Autexier and C. W. Greider, *Genes Dev.* **9**, 2227 (1995).
24. J. Prescott and E. H. Blackburn, *Genes Dev.* **11**, 528 (1997).
25. G. P. Harrison, M. S. Mayo, E. Hunter, A. M. Lever, *Nucleic Acids Res.* **26**, 3433 (1998); B. I. Klasens, H. T. Huthoff, A. T. Das, R. E. Jeeninga, B. Berkhout, *Biochim. Biophys. Acta* **1444**, 355 (1999).
26. T. M. Nakamura and T. R. Cech, *Cell* **92**, 587 (1998).
27. E. H. Blackburn, in *The RNA World*, R. F. Gesteland, T. R. Cech, J. F. Atkins, Eds. (Cold Spring Harbor Laboratory Press, Cold Spring Harbor, NY, 1999), pp. 609–636.
28. M. Zuker, *Science* **244**, 48 (1989).
29. M. A. Ansari-Lari, S. N. Jones, K. M. Timms, R. A. Gibbs, *Biotechniques* **21**, 34 (1996).
30. We thank R. Andino, C. Autexier, T. Cech, S. Chan, C. Gross, A. Krauskopf, J. Lin, Y. Mandel-Gutfreund, M. McEachern, S. Nautiyal, J. Shlomai, H. Wang, and H. Zehavi for critical reading of the manuscript and useful advice; the members of the Blackburn lab for stimulating discussions; and M. Lachance for kindly providing *Kluyveromyces* species. Supported by an NIH grant to E.H.B. (GM26259), a Human Frontier Science Program fellowship to Y.T. (LT-415/96), and an NIH training grant to T.B.F. (T32CA09270).

25 January 2000; accepted 15 March 2000

Promoter-Selective Properties of the TBP-Related Factor TRF1

Michael C. Holmes and Robert Tjian*

The TATA-binding protein (TBP)–related factor 1 (TRF1) is expressed in a tissue-restricted fashion during *Drosophila* embryogenesis and may serve as a promoter-specific recognition factor that can replace TBP in regulating transcription. However, bona fide target promoters that would preferentially respond to TRF1 have remained elusive. Polytene chromosome staining, chromatin immunoprecipitation, direct messenger RNA analysis, and transient cotransfection assays identified the *Drosophila* gene *tudor* as containing a TRF1-responsive promoter. Reconstituted in vitro transcription reactions and deoxyribonuclease I footprinting assays confirmed the ability of TRF1 to bind preferentially and direct transcription of the *tudor* gene from an alternate promoter. Thus, metazoans appear to have evolved gene-selective and tissue-specific components of the core transcription machinery to regulate gene expression.

Diverse mechanisms have evolved to regulate the spatial and temporal patterns of gene expression required for growth, differentiation, and response to environmental stimuli (*1*). Cell type–specific transcriptional activators that interact with enhancer DNA sequences to control programs of gene expression in metazoans have received much attention. In contrast, the general transcriptional apparatus has been viewed as a nonregulated "basal" component because the RNA polymerase II (Pol II) machinery was largely thought to be invariant in its composition or expression. However, these earlier studies did not anticipate the possibility that the Pol II machinery itself might display tissue-specific or gene-selective properties. In 1993, a novel TBP-related gene product, TRF1, was isolated from *Drosophila* and subsequently found to display properties expected of a cell type–specific TBP molecule (*2, 3*). In addition to being expressed in a tissue-restricted fashion, TRF1 was able to interact with TFIIA and TFIIB to form a Pol II preinitiation complex that accurately directs transcription in vitro. Polytene chromosome staining with an antibody to TRF1 revealed its association in vivo with a small subset of genes within the *Drosophila* genome. However, there was no evidence that TRF1 could differentially recognize distinct classes of promoters.

To identify promoters regulated by TRF1, we performed chromatin immunoprecipitation experiments with formaldehyde-treated SL2 cells (*4*). The *tudor* gene previously identified by TRF1 chromosome staining was specifically tested for TRF1 interaction. A 400–base pair (bp) fragment of the *tudor* promoter was probed by Southern hybridization with ^{32}P-labeled DNA prepared from the chromatin immunoprecipitations. As a control, we also probed a 1.7-kb fragment of the *Antennapedia* P1 promoter (AntP1). DNA sequences crosslinked and precipitated with TRF1 hybridized strongly to the *tudor* promoter fragment, whereas no signal was detected for the AntP1 fragment (Fig. 1, lanes 7 and 8). By contrast, DNA sequences coprecipitated with the transcription factor Adf-1 hybridized strongly to the AntP1 promoter but not the *tudor* promoter (Fig. 1, lanes 5 and 6). Adf-1 had been previously shown to regulate the expression of *Antennapedia* through the P1 promoter (*5*). Anti-TBP or control beads alone failed to precipitate either promoter fragment (Fig. 1, lanes 1 to 4). These studies taken together suggest that in vivo TRF1 associates selectively with DNA sequences within 500 bp of the *tudor* promoter.

To determine whether TRF1 could functionally modulate the expression of *tudor*, we

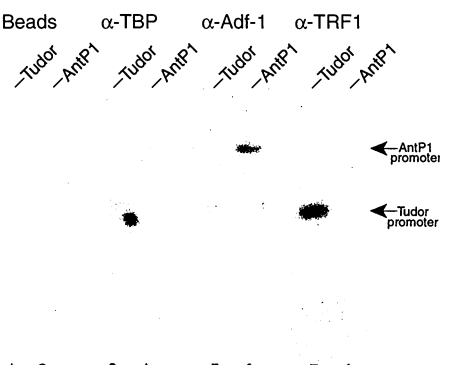

Fig. 1. TRF1 associates with the *tudor* core promoter in SL2 cells. DNA hybridization blots were probed with DNA isolated from chromatin immunoprecipitations of formaldehyde-treated SL2 cells. Each blot contained restriction fragments of the *tudor* and *Antennapedia* P1 (AntP1) promoters, which were separated by agarose gel electrophoresis and transferred onto Gene Screen Plus nylon membranes (NEN Life Science Products). Chromatin immunoprecipitations were carried out using antibodies to TBP (α-TBP), Adf-1 (α-Adf-1), or TRF1 (α-TRF1). As a negative control, mock immunoprecipitations were performed with protein A–Sepharose beads alone. On the α-TRF1 blot, the DNA crosslinked to TRF1 hybridized to the 400-bp *tudor* promoter fragment (lane 7), indicating that TRF1 binds a DNA sequence within 500 bp of the *tudor* core promoter in vivo. The DNA precipitated with TRF1 antibodies did not cross-react with the 1.7-kb AntP1 promoter fragment (lane 8). Arrows denote the positions of the *tudor* and AntP1 promoters on the blots. The DNA isolated in the Adf-1 immunoprecipitation hybridized to the AntP1 promoter fragment (lane 6) but not to the *tudor* promoter fragment (lane 5). The α-TBP and beads-only control immunoprecipitations (lanes 1 to 4) failed to efficiently precipitate either the *tudor* or AntP1 promoter fragments.

Howard Hughes Medical Institute, Department of Molecular and Cell Biology, University of California, Berkeley, CA 94720, USA.

*To whom correspondence should be addressed. E-mail: jmlim@uclink4.berkeley.edu